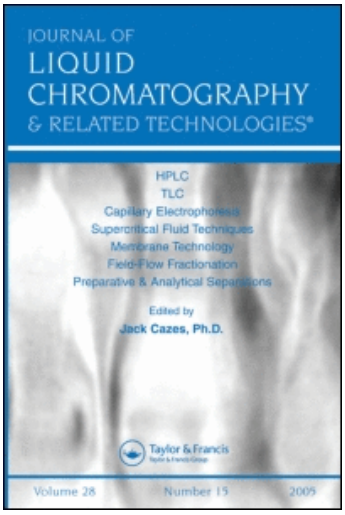

Journal of Liquid Chromatography & Related Technologies

Publication details, including instructions for authors and subscription information:
http://www.informaworld.com/smpp/title~content=t713597273

Estimating the Effect of Particle Surface Coatings on the Adsorption of Orthophosphate Using Sedimentation Field-Flow Fractionation

Jason Van Berkel[a]; Ronald Beckett[a]
[a] Department of Chemistry Monash University, CRC for Freshwater Ecology and Water Studies Centre, Australia

To cite this Article Van Berkel, Jason and Beckett, Ronald(1997) 'Estimating the Effect of Particle Surface Coatings on the Adsorption of Orthophosphate Using Sedimentation Field-Flow Fractionation', Journal of Liquid Chromatography & Related Technologies, 20: 16, 2647 — 2667
To link to this Article: DOI: 10.1080/10826079708005585
URL: http://dx.doi.org/10.1080/10826079708005585

J. LIQ. CHROM. & REL. TECHNOL., 20(16 & 17), 2647–2667 (1997)

ESTIMATING THE EFFECT OF PARTICLE SURFACE COATINGS ON THE ADSORPTION OF ORTHOPHOSPHATE USING SEDIMENTATION FIELD-FLOW FRACTIONATION

Jason Van Berkel, Ronald Beckett*

CRC for Freshwater Ecology and Water Studies Centre
Department of Chemistry
Monash University
P. O. Box 197
Caulfield East, Vic. 3145, Australia

ABSTRACT

The adsorption behaviour of pollutants to natural colloids is affected by particle surface coatings such as hydrous iron oxides, manganese oxide and natural organic matter (NOM).

Sedimentation field-flow fractionation (SdFFF) was used to determine surface adsorption density distributions (SADD) for ^{33}P-labelled orthophosphate onto suspended colloidal samples from the Peel River (NSW, Australia). The surface adsorption density (SAD) is the amount of pollutant adsorbed per unit area of particle surface. For a homogeneous particle sample, the SAD is expected to be constant. The SAD for the Peel River sample increased significantly with particle size, which may be due to changes in particle shape, mineralogy, or the nature of the surface coatings.

Scanning electron microscopy (SEM) was used to determine particle shape by examining separated fractions. The SAD was shape corrected using recently developed theory.

Analysis of the sample suggested particle shape was fairly constant and, thus, did not influence the trends in the SAD significantly.

In light of the SEM analysis, it was more likely the nonconstant SAD was associated with a change in mineralogy or surface coating composition. The purpose of this work was to investigate the effect of these surface coatings on orthophosphate adsorption. The particle surface coatings were selectively removed from the colloidal particles by chemical treatment and the effects on orthophosphate adsorption were investigated. Removal of the iron oxyhydroxide coatings decreased the SAD slightly but removal of NOM coatings increased orthophosphate adsorption substantially.

INTRODUCTION

Many processes which determine the behaviour of pollutants in natural waters occur at the surfaces of colloidal particles. Consequently, the study of colloid-nutrient interactions is an important part of ongoing research into the causes of algal blooms. Iron and manganese hydroxy oxides and natural organic matter (NOM) can exist in nodules, concretions, cement between particles or simply as coatings on particle surfaces (See Fig. 1).

These oxides are excellent scavengers of trace metals (e.g. Zn^{2+}, Cu^{2+}) and nutrients (e.g. PO_4^{3-}).[1] Therefore, the adsorption of pollutants onto these surfaces is a major factor in determining their reactivity and fate (transport, deposition) in aquatic systems. The pollutants may then concentrate in the bottom sediments at certain locations such as reservoirs and estuaries with serious ecological and human health implications.[2]

This paper reports a study in which different extractants are used to remove either iron oxide or NOM surface coatings and the resultant effect on orthophosphate adsorption and particle chemical composition was determined. The widely applied extraction sequence of Tessier and coworkers[1] has been modified by various authors; a version by Kersten and Förstner[3] claims to differentiate between the easily and moderately reducible components of surface coatings. This procedure was used as a basis for this research. According to

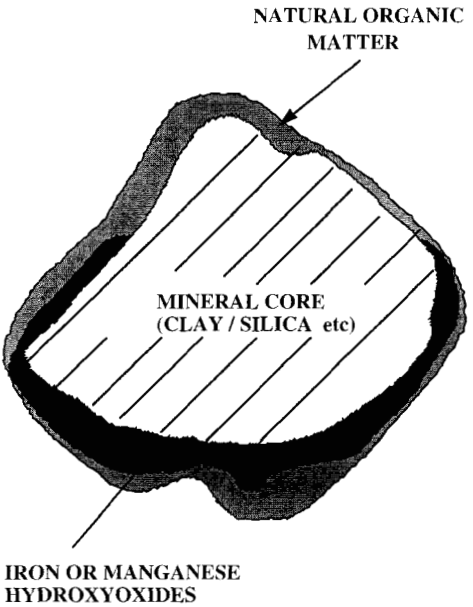

Figure 1. Schematic illustration of a natural suspended aquatic colloid, showing several types of surface coatings.

Kersten and Förstner,[3] 0.1 M oxalate extracts the moderately reducible surface coatings such as the amorphous Fe and Mn oxides. The effectiveness of oxalate arises from the low redox potential (-0.63V) and its ability to coordinate and form moderately stable metal complexes in weakly acidic solution, leading to the stripping of hydrous metal oxide layers.[4] However, it should be noted that these extraction methods are not absolutely selective for specific metal surface coatings and can also be influenced by the time of exposure and by the ratio of particulate matter to volume of extractants.[5]

Tessier et al.[1] evaluated the optimum extraction time for the removal of the Fe and Mn oxides. The results indicated the extraction was essentially complete after 6 hours. Longer times increased the possibility of attacking organic matter and residual solids within the crystalline structures.

In order for the organic matter to be successfully extracted, it must be oxidized to form carbon dioxide and water. This can be achieved with hydrogen peroxide. It is postulated that the organic matter competes with nutrients such as orthophosphate for adsorption sites. Once the organic matter

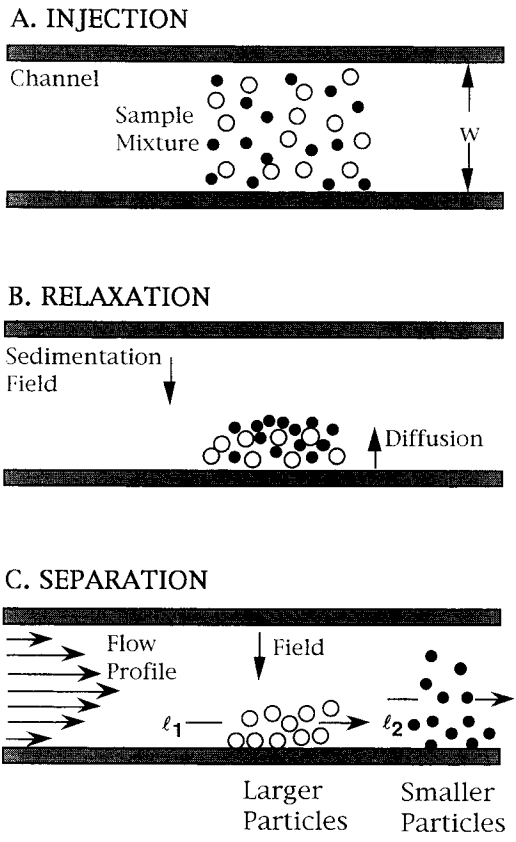

Figure 2. Cross-section of the SdFFF channel, showing different stages of an SdFFF analysis (a) injection, (b) relaxation, and (c) separation.

has been extracted, thus exposing the reactive hydrous Fe and Mn oxides surfaces, the amount of adsorption onto these surfaces is expected to increase. In previous publications, Beckett and coworkers have developed physical and chemical characterisation methods[6] based on sedimentation field-flow fractionation (SdFFF) for studying pollutant-colloid interactions.[2] SdFFF is a set of high resolution liquid chromatography-like elution methods used for separating and sizing colloidal particles.[7-10]

To perform a SdFFF separation, the sample is injected into the channel through a septum or injection valve (see Fig. 2a). An external centrifugal field is then applied at right angles to the ribbon-like channel which sits within a

centrifuge basket (see Fig 2b). This field forces the particles of different effective masses to accumulate at different average positions relative to the accumulation wall. This depends on how strongly the particles interact with the field and also their diffusivity.[11] This process is called relaxation and is usually achieved during a stop-flow period.

After the stop-flow period, the carrier liquid flow is turned on and the run begins. The carrier flow develops a parabolic profile within the channel with the highest flow rates in the centre of the channel and flow velocities approaching zero near the channel walls. The particles with a larger effective mass will have more compressed sample clouds (i.e., a smaller ℓ) and will be swept down the channel by the carrier flow at a lower average velocity than the smaller particles. Thus, the smallest particles will elute first (See Fig. 2c).

When an inductively coupled plasma-mass spectrometer (ICP-MS) is coupled to a SdFFF instrument, element-based size distributions and element molar ratio plots can be calculated.[7] This elemental data is valuable in interpreting mineralogy or surface coating changes across the size distribution.

The SdFFF approach is also amenable for studying pollutant-colloid binding.[2] Radiolabelled orthophosphate can be adsorbed onto the colloidal particles that can then be separated and sized with SdFFF. Fractions can be collected throughout the run and the radioactivity measured as a function of particle size. This adsorption data can also be used to determine a surface adsorption density distribution (SADD) plot. An SADD plot graphs the amount of pollutant adsorbed per unit area of particle surface as a function of particle size. For a homogeneous sample, the SADD plot should be constant across the entire size distribution. However, due to the complex nature of colloid particles (e.g., shape, mineralogy and surface coatings), a constant SADD plot is not always observed. It is the purpose of this paper to investigate the role of surface coatings on orthophosphate adsorption and their influence in generating nonconstant SADD plots.

THEORY

Sedimentation Field-Flow Fractionation

The sample is passed through a UV detector operating at 254 nm as it elutes from the channel. The retention ratio, R, and retention parameter λ for a constant field normal FFF run is obtained from the elution volume V_r and the channel void volume V^0 according to the general expression for normal mode

FFF separations:

$$R = \frac{V^0}{V_r} = 6\lambda\left(\coth\frac{1}{2\lambda} - 2\lambda\right) \quad (1)$$

where $\lambda = \ell/w$, with ℓ being the mean cloud thickness and w being the channel thickness. For constant field SdFFF runs, the equivalent spherical diameter, d can be calculated from λ provided the density difference between the particle and carrier liquid, $\Delta\rho$ is known.[7]

$$d = \sqrt[3]{\frac{6kT}{\pi\omega^2 rw\Delta\rho\lambda}} \quad (2)$$

where k is the Boltzmann constant, T the absolute temperature, ω the centrifuge speed (radians s^{-1}) and r the centrifuge radius.

A field decay program developed by Williams and Giddings[12] can be used for samples with broad size distributions. Initially, the centrifuge speed ω_0 is held constant for a lag period t_1, after which the field speed decays according to:

$$\omega = \omega_0\left(\frac{t_1 - t_a}{t - t_a}\right)^4 \quad (3)$$

where t_a is a constant which along with t_1 controls the rate of field decay and t is the run time. This method can be used to prevent excessively long retention times for the larger particles, while still enabling the smallest particles to elute far enough from the void peak.

Fractograms

A fractogram is a plot of UV detector response versus elution time, where the UV signal is used as a surrogate for the mass concentration of particles in the eluent. Although the UV attenuation is affected to some extent, by the particle size according to the Mie theory, this has not been taken into account for this work. However, it has been observed that the UV based fractogram is often similar to the major element fractogram determined by the use of an inductively coupled plasma-mass spectrometer (ICP-MS) detector, which suggests that this Mie purturbation does not affect the particle size distribution substantially.[7]

Thus, the fractograms depict a plot of our estimate of the mass concentration of particles (dm^c/dV) measured by a UV detector, operating at 254 nm, versus elution time (t_r) or volume (V_r).[2] The y-axis is, therefore, shown in arbitrary units.

The mass concentration of an element E can be determined by using a sensitive analytical instrument such as an ICP-MS. After passing the sample through the UV detector, it is fed into the ICP-MS and an ion current I_E is generated, which is a measure of the mass concentration of elements eluting (i.e. dm^c_E/dV_r).

Mass Based Size Distribution

The particle size distribution represents the amount of material contained within different size ranges. It is a plot of dm^c/dd versus d, where m^c is the cumulative mass of sample eluted up to a given point and d the particle diameter at that point. The equivalent spherical diameter of a particle can be calculated by combining Equations 2 and 3. The run must be assumed to be made up of a large number of constant field increments stepping down from ω_0 as the field decays. The volume axis of the fractogram is divided into small volume increments of δV_r and the following expression is used:

$$\frac{dm^c{}_{(i)}}{dd_i} = \left\{ \left(\frac{dm^c{}_{(i)}}{dV_{r(i)}} \right) \times \left(\frac{\delta V_{r(i)}}{\delta d_{(i)}} \right) \right\} \propto UV_{(i)} \times \frac{\delta V_{(i)}}{\delta d_{(i)}} \qquad (4)$$

where $dm^c{}_{(i)}/dV_{r(i)}$ is the value of the fractogram ordinate (assumed to be proportional to the UV detector response) at the midpoint of a given volume increment $\delta V_{r(i)}$, and $\delta d_{(i)}$ the diameter increment corresponding to the same increment in V_r. An element based size distribution can be calculated similarly using the ICP-MS data (I_E).

Surface Adsorption Density Distribution

The amount of pollutant adsorbed can be measured by collecting samples at various elution times and measuring the pollutant concentration. In suitable cases, this can be achieved using radiolabelled compounds and measuring the radioactivity in a scintillation counter. The amount of pollutant adsorbed per unit mass of particle at any point (i) along the elution time or volume axis is:

$$\frac{dm^{c}_{P(i)}}{dm^{c}_{(i)}} = \left\{ \left(\frac{dm^{c}_{P(i)}}{dV_{r(i)}} \right) / \left(\frac{dm^{c}_{(i)}}{dV_{r(i)}} \right) \right\} \propto \frac{DPM_{(i)}}{UV_{(i)}} \quad (5)$$

where $DPM_{(i)}$ is the ß activity in disintegrations per minute per mL of eluent and $m^{c}_{P(i)}$ is the cumulative mass of the adsorbed pollutant P eluted up to elution volume $V_{r(i)}$. For spherical particles the particle area ($\delta A^{c}_{(i)}$) in an increment of elution volume ($\delta V_{r(i)}$) is given by $6\delta m^{c}_{(i)}/d_{(i)p}$. Thus, if constant spherical shape and density is assumed, a surface adsorption density distribution can be calculated utilizing equation 5. The expression for this sphere based surface adsorption density becomes:

$$\left(\frac{dm^{c}_{P(i)}}{dA^{c}_{(i)}} \right)_{sphere} = \left\{ \left(\frac{dm^{c}_{P(i)}}{dm^{c}_{(i)}} \right) \times \left(\frac{\delta m^{c}_{(i)}}{\delta A^{c}_{(i)}} \right) \right\} \propto \frac{DPM_{(i)}}{UV_{(i)}} \times d_{(i)} \quad (6)$$

If there is a change in particle morphology to a more nonspherical shape, the amount of pollutant adsorbed per unit area would be underestimated. For example, a disc- or plate-like particle of the same mass as a spherical particle would have a larger surface area. A geometric expression has been developed for the ratio of surface areas of a coeluting disc (A_d) and sphere (A_s) in terms of the diameter ratio d_d/d_s where d_d is the equivalent circular cross-sectional diameter of the disc or rod and d_s is the diameter of a sphere with the same volume.[13] The expression is as follows:

$$\frac{A_d}{A_s} = \frac{1}{2}\left(\frac{d_d}{d_s} \right) + \frac{2}{3}\left(\frac{d_s}{d_d} \right) \quad (7)$$

The specific surface area of a plate or rod is underestimated the more its shape deviates from a sphere. The SADD plot can be corrected by incorporating the above expression into Equation 6.

At each point i along the distribution, the true SAD for the nonspherical sample ($(dm^{c}_{P(i)}/dA^{c}_{(i)})_{sample}$) will be given by:

$$\left(\frac{dm^{c}_{P(i)}}{dA^{c}_{(i)}} \right)_{sample} = \left(\frac{dm^{c}_{P(i)}}{d\left(A^{c}_{(i)}\right)} \right)_{sphere} / \frac{1}{m}\sum_{j=1}^{m}\left(\frac{A_d}{A_s} \right)_{(j)} \quad (8)$$

where A_d/A_s is the averaged ratio for the m particles examined by scanning electron microscopy (SEM) in the sample collected at point i along the fractogram. SEM is used to measure d_d and d_s is calculated from the SdFFF equations.[13]

Element Content of Particles

The amount of Fe per unit mass of particle ($dm^c_{Fe(i)}/dm^c_{(i)}$) at any point (i) along the elution time or volume axis can be calculated similarly to $dm^c_{P(i)}/dm^c_{(i)}$ (see Equation 5). The Fe concentration in the eluent $[Fe]_i$ can be measured by coupling an inductively coupled plasma-mass spectrometer (ICP-MS) to the SdFFF instrument. The expression is:

$$\frac{dm^c_{Fe(i)}}{dm^c_{(i)}} = \left(\frac{dm^c_{Fe(i)}}{dV_{r(i)}}\right) / \left(\frac{dm^c_{(i)}}{dV_{r(i)}}\right) \propto \frac{[Fe]_{(i)}}{UV_{(i)}} \qquad (9)$$

EXPERIMENTAL

Sample Collection

A sample containing suspended particulate matter was collected from the Peel River (New South Wales, Australia) just before it flowed into Chaffey Reservoir. The Peel River is a small urban stream which was dammed nearly 20 years ago to form Chaffey Reservoir. The latitude is about 31°20'S and the annual average inflow is 6.0×10^7 m^3. The sample was pumped through a continuous flow centrifuge to remove particles larger than 1 μm in size.[14] The filtrate (<1 μm) was then concentrated 100-fold using tangential flow filtration with 0.2 μm Millipore polysulphone membranes. The concentrate was refrigerated at 4°C and sonicated prior to separation by SdFFF.

Extraction Procedure

The above concentrated colloid sample was split into 3 equal subsamples of 0.5 mL volumes. 50 μL of 0.2 M ammonium oxalate (pH 3) was added to one subsample, 50 μL of 3% hydrogen peroxide was added to the second subsample, and the third subsample did not receive any extractants and was used as the control sample.

Each sample was stored at 4°C for 6 hours after which they were centrifuged to remove the supernatant and washed with 0.05% sodium dodecylsulphate (SDS). The samples were spun down in a centrifuge and washed with SDS two more times to remove all traces of the extractants and products from the reactions with the surface coatings.

Orthophosphate Adsorption

^{33}P labelled orthophosphate in dilute hydrochloric acid (370 MBq/mL) was obtained from the Australian Nuclear Science and Technology Organisation (ANSTO). The stock ^{33}P solution was diluted to 740 kBq/mL. At the time of injection into the sample concentrates the ^{33}P activity had decayed to 500 kBq/mL, as estimated from the decay rate law and length of storage. Ten mL of $^{33}PO_4^{3-}$ (500 kBq/mL) was injected onto 50 μL of the concentrated colloid samples and allowed to stand for 24 hours before separation by SdFFF.

Fractions were collected every 5 minutes as the particles eluted from the SdFFF. 0.5 mL of each collected fraction was added to 3.5 mL of scintillant (Ultima Gold), shaken and the ß activity measured for 10 minutes. The counts per minute (CPM) was recorded and, from this data, disintegrations per minute (DPM) per mL was computed.

Sedimentation Field Flow Fractionation

Apparatus

The SdFFF was similar to the basic systems described by Giddings and coworkers and available from FFFractionation LLC (Salt Lake City, Utah, USA), but modified as described in Van Berkel and Beckett.[12] The channel was made by clamping two concentric nickel-chromium rich alloy (Hastalloy) rings together with a 0.0254 cm mylar spacer, in which the channel shape had been cut out, sandwiched in between. There were two systems used. System 1 was used for the adsorption experiments and system 2 was coupled to an inductively coupled plasma-mass spectrometer (ICP-MS) to determine chemical composition of the particles. The channel length and breath for both systems was 89.1 cm long (inlet to outlet) and 2.15 cm respectively. The void volume was 4.91 mL and 2.5 mL for system 1 and 2, respectively. The channels were coiled to fit within a centrifuge basket. The radii of the channels were 15.1 cm and 15.5 cm for system 1 and system 2, respectively. O-rings were fitted at the axle ends to allow liquid to flow through the channel as the centrifuge rotates.

The centrifuge was powered by a DC motor (Baldor permanent magnet servomotor) and the speed controlled by in-house field-decay software. The carrier liquid was pumped through the channel by a Milton Roy ConstaMetricIII metering pump. The outlet stream was passed through an LDC Milton Roy SpectroMonitor variable wavelength detector operating at 254 nm. The samples were collected by an ISCO Retriever 500 fraction collector.

FFF Run Parameters

100 μL and 30 μL of sample concentrate was injected into systems 1 and 2, respectively, using a microsyringe. The samples were relaxed for 10 minutes at 1500 rpm under stop-flow conditions. For system 1, t_1 was 5.6 minutes and t_a was -43 minutes. For system 2, t_1 was 3.5 minutes and t_a was -28 minutes. The field was reduced using the power program to a minimum 20 rpm. The liquid carrier used for both systems was 0.05% w/v sodium dodecylsulphate (SDS) and 0.02% w/v sodium azide. The flow rates were 2 mL/min and 1 mL/min for system 1 and 2, respectively. Detector sensitivity was 0.02 a.u.f.s.

Scanning Electron Microscopy (SEM)

An Hitachi S-2300 model SEM was used to determine the shapes of the colloidal particles and to verify the accuracy of the SdFFF separations. The 10 mL fractions collected every 5 mins were filtered through either a 0.05 μm Nucleopore filter for sizes less than 0.1 μm or a 0.1 μm Nucleopore filter for sizes larger than 0.1 μm. The filters were cut (approximately 0.5 cm x 1 cm) and attached to an aluminium stub. For SEM analysis, the filters were coated with platinum.

Inductively Coupled Plasma-Mass Spectrometer Apparatus (ICP-MS)

The SdFFF was directly coupled to a VG Plasmaquad ICP-MS in order to obtain high resolution element distributions as a function of particle size. By using a t-piece after the UV detector and a peristaltic pump attached to the v-groove nebulizer of the ICP-MS, about half of the eluent from the SdFFF could flow into the ICP-MS, and the remainder could be collected with a fraction collector or go directly to waste. The internal standards present in the sodium dodecylsulphate (SDS) carrier were indium and cesium. These were used to make corrections for noise and drift. The ICP-MS run conditions were as follows: mass range 23.5 to 210.41 a.m.u.; number of scan sweeps 100 and the instrument operated in pulse-counting mode. Calibration was achieved using a

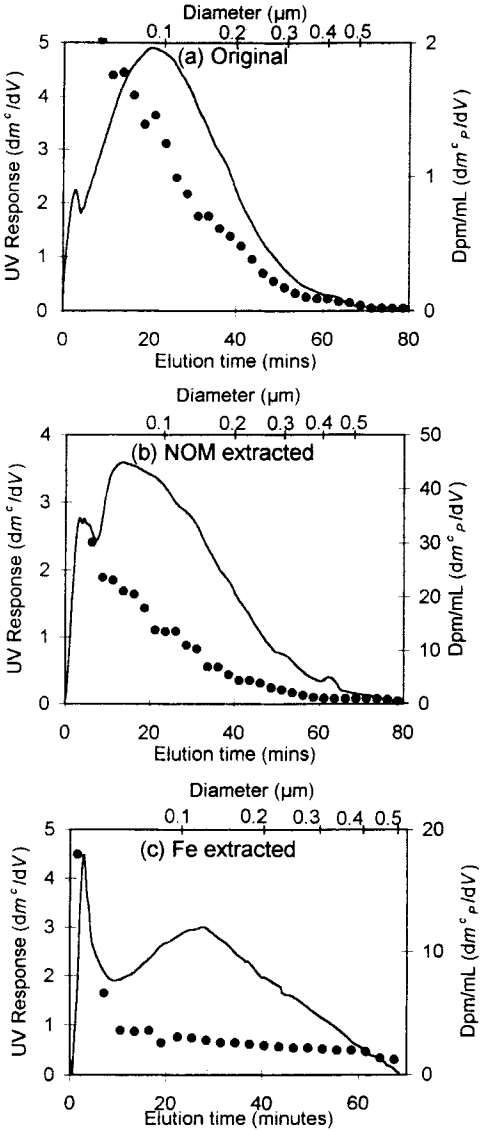

Figure 3. SdFFF fractograms (system 1) of Peel River colloids with adsorbed radiolabelled orthophosphate. The solid lines give the UV detector response (arbitrary units) and the points give the radioactivity (Dpm/mL) in the effluent. (a) original river sample, (b) natural organic matter extracted sample, and (c) hydrous iron oxide extracted sample.

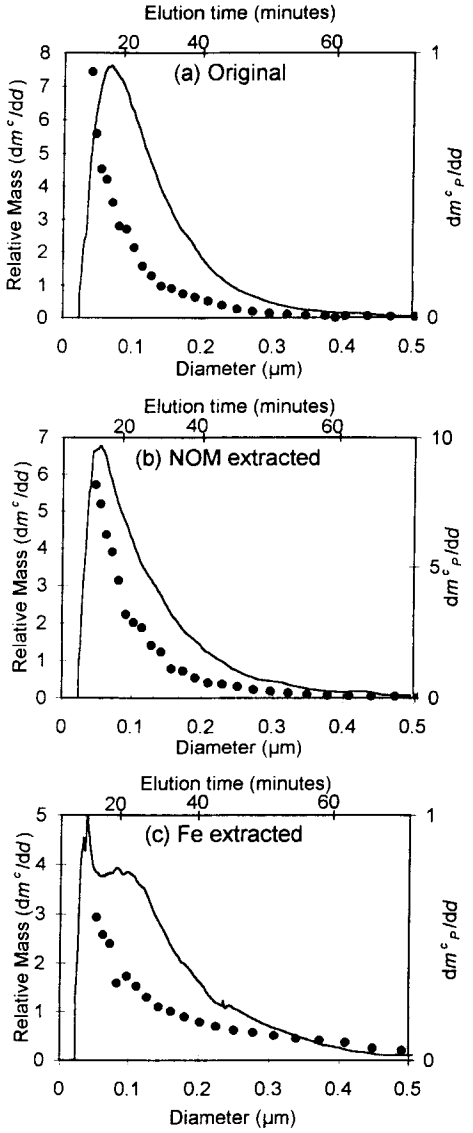

Figure 4. Particle mass based and adsorbate based size distributions. The solid lines give the relative mass of the particles and the points give the amount of orthophosphate adsorbed (both in arbitrary units). (a) original river sample, (b) natural organic matter extracted sample, and (c) hydrous iron oxide extracted sample.

standard solution containing 200 ppb Fe and other elements. This standard was diluted two-fold, four-fold and eight-fold with SDS/azide carrier and the solutions analysed by the ICP-MS prior to each run. An Excel, (Microsoft) macros program was used to perform element by element drift corrections and compute the element concentrations based on ion currents obtained for the above solution standards.

RESULTS AND DISCUSSION

Fractograms and Size Distributions

The raw UV detector and scintillation counter based fractograms, together with the computed particle size distribution for each sample, are shown in Figs. 3 and 4. All samples show a relatively narrow size distribution from 0.05-0.3 μm. The tail does extend to 0.5 μm but, since the signal is small from 0.3-0.5 μm, it is more difficult to analyse trends in this region (see Figs. 4a, b, and c). The size distributions for the NOM extracted sample did not change significantly from the original colloid sample (see Figs. 4a and b). The Fe oxide extracted sample showed a slight broadening of the particle size distribution (see Figs. 4a and c).

The $^{33}PO_4^{3-}$ adsorption experiments show that most orthophosphate is taken up by the smaller particles (see Figs. 4a, b and c). This is due to both the greater mass of material in the smaller size fractions and to the increase in the specific surface area of these particles as particle size decreases.

Analysis of Chemical Composition by SdFFF-ICP-MS

The new hyphenated technique of SdFFF-ICP-MS has excellent potential for determining any changes in particle mineralogy or surface coatings across the size distributions.[7] Fig. 5 shows the iron content of the particles as a function of particle diameter. For the original sample, the amount of iron per unit mass of particle (dm^c_{Fe}/dm^c) increases significantly with increasing particle size (see Fig. 5a). The Fe concentration increased by a factor of 2 over the size range 0.15 to 0.5 μm. The iron can be in either of the following forms: (a) within the solid mineral lattice core of the colloidal particles, or (b) as hydrous iron oxide coatings on the surface of the particles (see Fig. 1). After the extraction of the hydrous iron oxide surface coatings with ammonium oxalate,

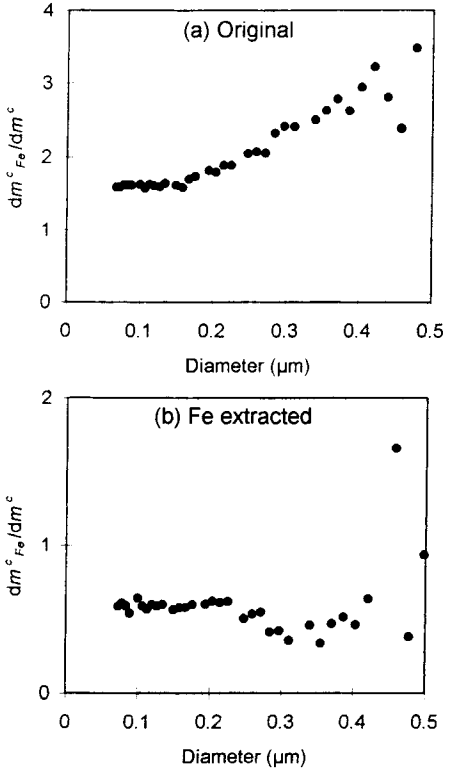

Figure 5. The concentration of Fe within the particles (dm^c_P/dA^c) in arbitrary units), plotted as a function of particle diameter. (a) original river sample and (b) hydrous iron oxide extracted sample.

the iron content plot was constant across the size distribution (see Fig. 5b). This suggests that the iron concentration within the mineral core of the particles is constant across the size distribution. This probably implies that the particle mineralogy remains unchanged.

The amount of iron found on the surfaces can be determined by the difference between the two samples. Figure 6 shows such a plot of the amount of iron associated with the particle coatings per unit area of particle surface. The trend is nonconstant, it increases substantially with increasing particle size (0.15-0.5 μm) indicating the iron surrounding the larger particles is more densely coated with hydrous iron oxides than the smaller particles.

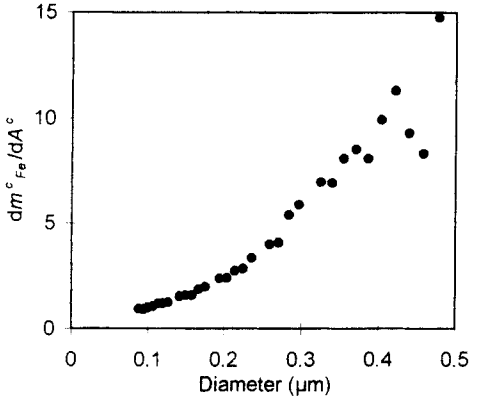

Figure 6. The calculated Fe surface coating density distribution plots (dm^c_P/dA^c versus diameter).

It should be noted that in this work the influence of particle size on the UV attenuation has been neglected and this could have some effect on the coating thickness distribution trend. However, as noted earlier, we believe this is likely to be a small effect since it was observed that the UV and Al based fractograms were very similar (data not included in this paper). In addition, if the UV signal increases with diameter, as may be expected in this size range ($d \approx \ell$), this would further increase the rate of increase of coating thickness with particle diameter.

Surface Adsorption Density Distributions

The surface adsorption density distribution (SADD) plots are shown in Fig. 7. The SADD plots are calculated from the UV and DPM shown on the fractograms in Figs. 3a, b, and c. The SADD plots for all samples were nonconstant. The plots showed an increase in SAD as particle size increased from 0.1 to 0.5 μm. This suggests the larger sized particles adsorbed more orthophosphate per unit area of particle surface than the smaller particles (see Fig 7a). This trend could be influenced by changes in particle shape, mineralogy or surface coatings. The particle shape corrected SAD (dm^c_P/dA^c_{sample}) is calculated using equation 8 as previously discussed. The closed circles represent the SAD values before particle shape correction (dm^c_P/dA^c_{sphere}) and the open circles represent the SAD values after particle shape correction (dm^c_P/dA^c_{sample}). It appears that changes in particle shape do

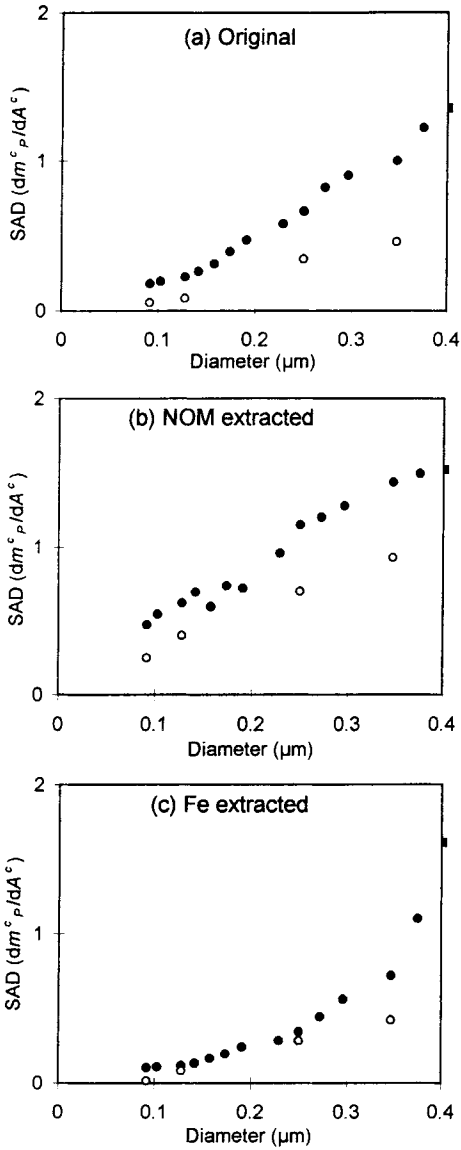

Figure 7. The effect of particle shape correction on the calculated orthophosphate surface adsorption density distribution (SADD) of a river colloid sample. The closed circles give the amount of orthophosphate adsorbed per unit area of particle surface (arbitrary units) assuming all particles are spherical and the open circles are corrected for changes in shape. (a) original river sample, (b) natural organic matter extracted sample, and (c) hydrous iron oxide extracted sample.

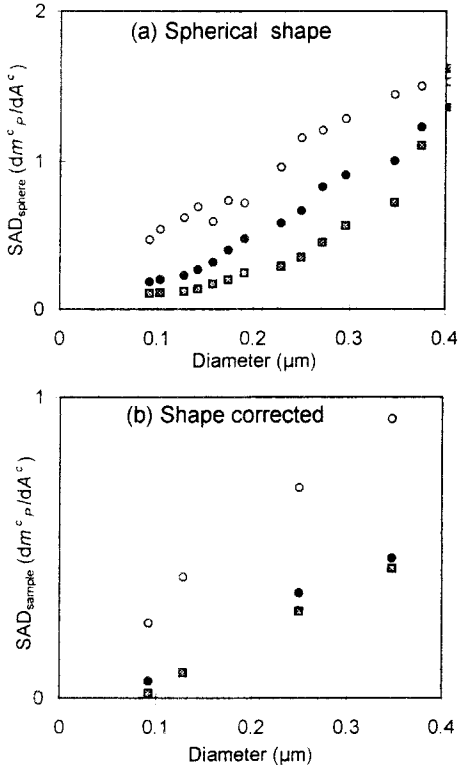

Figure 8. The effect of surface coating extraction on the orthophosphate surface adsorption density distribution (SADD) plots of a river colloid sample. (a) no shape correction and (b) after shape correction. The black circles refer to the original river sample, the open circles are for the natural organic matter extracted sample and the grey squares are for the hydrous iron oxide extracted sample.

not affect the trends in the SADD plots for these samples, even though there was a shift in the absolute values of the surface adsorption density in each case. The nonconstant SADD plot for the control sample is most likely associated with the increased surface coating density of iron around the larger colloidal particles as previously discussed (see Fig. 6).

Effect of Particle Surface Coatings on the SADD Plots

The SADD plot trends remained nonconstant for all samples even after surface coating extraction (see Figs. 7b and c, 8a and b).

The SAD for the Chaffey Dam sample after natural organic matter extraction increased about four-fold over the size range 0.1 to 0.5 μm. Thus, the presence of natural organic matter inhibits the adsorption of orthophosphate to the particles. The extraction of the organic matter apparently exposed the hydrous iron oxide surfaces underneath.

As previously discussed, since the larger particles contained more iron on their surface (see Fig. 6), this could explain the observed nonconstant SAD trend in this case (see Figs. 7b, 8a, and b).

Surprisingly, the attempted removal of the hydrous iron oxide coatings with sodium oxalate resulted only in a small decrease in the surface adsorption density and the shape corrected SADD plot retained its positive gradient (i.e., increasing SAD with increasing particle size).

Unfortunately, in these preliminary experiments we cannot discount the possibility that the extraction conditions did not remove all of the hydrous iron oxide coatings (see Figs 7c, 8a, and b). To investigate this possibility, further work needs to be conducted using more vigorous extraction procedures while carefully monitoring the extent of removal of the iron coatings.

CONCLUSION

The amount of orthophosphate adsorbed per unit area of particle surface as a function of particle size was found to be nonconstant for a Peel River suspended colloid sample. This observed nonconstant SAD trend is apparently associated with an increased surface coating density of hydrous iron oxides with increasing particle size.

The extraction of iron and natural organic matter did not change this observed nonconstant SAD trend. However, the amount of orthophosphate adsorbed per unit area of particle surface decreased slightly after iron surface coating extraction and increased substantially after organic matter surface coating extraction.

These preliminary experiments demonstrate a new methodology which combined previously developed SdFFF-ICP-MS and SdFFF-adsorption techniques to give new insights into the role of surface coatings on natural particles in biogeochemical processes in aquatic ecosystems. The methods introduced here should also be applicable to other industrial and biological samples.

ACKNOWLEDGMENTS

Jason van Berkel was supported by a CRCFE postgraduate scholarship. This research was supported by the CRCFE and the Australia Research Council. We also acknowledge the great contribution of Prof J. Calvin Giddings whose leadership and encouragement over the past 13 years have been invaluable in establishing this research program.

REFERENCES

1. A. Tessier, P. G. C Campbell, M. Bisson, Anal. Chem., **51(7)**, 844-851 (1979).

2. R. Beckett, D. M Hotchin, B. T Hart, J. Chromatogr., **517**, 435-447 (1990).

3. M. Kersten, U. Förstner, Wat. Sci. Tech., **18**, 121-130 (1986).

4. W. F Pickering, CRC Crit. Rev. Anal. Chem., Nov: 233-266 (1981).

5. U. Förstner, **Contaminated Sediments: Lecture Notes on Environmental Aspects of Particle-Associated Chemicals in Aquatic Systems**, Springer-Verlag., New York, 1989.

6. R. Beckett, G. Nicholson, B. T Hart, M. Hansen, J. C Giddings, Water Res., **22**, 1535-1545 (1988).

7. D. M Murphy, J. R. Garbarino, H. E. Taylor, B. T. Hart, R. Beckett, J. Chromatogr., **642**, 459-467 (1993).

8. J. C. Giddings, Chem. Eng. News., **66**, 34-45 (1988).

9. R. Beckett, G. Nicholson, D. M. Hotchin, B. T. Hart, Hydrobiologia., **235/236**, 697-710 (1992).

10. R. Beckett, B. T. Hart, "Use of Field-Flow Fractionation Techniques to Characterize Aquatic Particles, Colloids and Macromolecules," in **Environmental Particles**, J. Buffle, Ed., Vol. 2, Lewis Publishers, Boca Raton, FL, 1993, pp. 165-205.

11. J. C. Giddings, Science., **260**, 1456-1465 (1993).

12. P. S. Williams, J. C. Giddings, Anal. Chem., **59**, 2038-2044 (1987).

13. J. Van Berkel, R. Beckett, J. Chromatogr., **733**, 105-117 (1996).

14. G. B. Douglas, R. Beckett, B. T. Hart, Hydrological Processes., **7**, 177-191 (1993).

Received February 2, 1997
Accepted April 16, 1997
Manuscript 4455